Journal of the American College of Cardiology Vol. 49, No. 3, 2007

Published by Elsevier Inc.
ISSN 0735-1097/07/$32.00
doi:10.1016/j.jacc.2006.08.056

Endocardial and Epicardial Repolarization Alternans in Human Cardiomyopathy

Evidence for Spatiotemporal Heterogeneity and Correlation With Body Surface T-Wave Alternans

Raja J. Selvaraj, MD, Peter Picton, MENG, Kumaraswamy Nanthakumar, MD, FRCPC, Susanna Mak, MD, PHD, FRCPC, Vijay S. Chauhan, MD, FRCPC

Toronto, Canada

Objectives The aim of this study was to define the spatiotemporal distribution of intracardiac alternans and its relationship to body surface alternans in humans.

Background Spatial heterogeneity of alternans exists in the animal heart owing to nonuniform calcium cycling and restitution kinetics. Patients with cardiomyopathy manifest similar myocardial substrate, which might influence the distribution of intracardiac alternans and its projection onto the body surface.

Methods Repolarization alternans was simultaneously measured from unipolar electrograms in the right ventricular endocardium, left ventricular (LV) epicardium, and the surface electrocardiogram in patients with cardiomyopathy ($n = 14$, LV ejection fraction 29 ± 2%) during atrial pacing at cycle length (CL) 800, 600, and 500 ms. Alternans was determined from the entire JT interval as well as the early, mid, and late JT interval with spectral analysis.

Results Alternans was not uniformly distributed within the heart, with alternating and nonalternating myocardial segments lying adjacent to one another. A greater number of epicardial sites exhibited alternans than endocardial sites at CL 600 ms. Temporal heterogeneity in alternans was present along the JT interval, and apical segments had proportionately less alternans in the late JT interval than mid or basal segments, resulting in apicobasal alternans heterogeneity in late JT interval. Discordant alternans was seen in 5 patients confined to the epicardium. Patients with surface alternans had a greater proportion of intracardiac sites with alternans when compared with those patients without surface alternans.

Conclusions Spatiotemporal heterogeneity and discordant alternans are evident in patients with cardiomyopathy. Greater spatial distribution of intracardiac alternans is associated with measurable body surface alternans. (J Am Coll Cardiol 2007;49:338–46) © 2007 by the American College of Cardiology Foundation

Repolarization alternans describes the beat-to-beat alternation in the shape or amplitude of the ST segment and T wave. In humans, repolarization alternans has been well

See page 347

characterized from the body surface and it has been shown to exhibit heart rate dependency (1), phase reversal (2), and temporal heterogeneity along the JT interval (3). Body surface T-wave alternans (TWA) predicts total mortality and nonfatal ventricular arrhythmias in patients with cardiomyopathy and is emerging as an important prognostic marker in this clinical setting (4,5). However, the origin of body surface TWA within the human heart has not been well defined. A limited number of reports have measured intracardiac alternans with spectral analysis of the unipolar JT interval recorded from a single ventricular site (6,7). These studies provide little information about the regional distribution of intracardiac alternans and its relationship to body surface TWA.

The spatial distribution of alternans is not uniform in the animal heart (8,9). In particular, arrhythmogenic repolarization gradients can develop during discordant alternans where anatomically distinct myocardial segments alternate out of phase from one another (10). Important mechanisms driving this spatial heterogeneity include nonuniform intracellular calcium cycling (8,11) and restitution kinetics (12).

From the Division of Cardiology, University Health Network and Mount Sinai Hospital, Toronto, Canada. Support was received from the Heart and Stroke Foundation of Canada (T5381) and the Canadian Foundation for Innovation (7498, to Dr. Chauhan).

Manuscript received May 23, 2006; revised manuscript received July 24, 2006, accepted August 14, 2006.

In humans, abnormalities in intracellular calcium cycling exist in diseased myocardial segments (13), and restitution kinetics have been shown to exhibit regional heterogeneity (14), which might provide the substrate for nonuniform alternans. The temporal distribution of alternans might also vary with disease states. In an animal model of ischemia, alternans is apparent in the first half of the T wave (15), whereas in patients with myocardial substrate for ventricular arrhythmias, alternans is seen later during repolarization (3).

Therefore, we hypothesized that the spatial and temporal distribution of intracardiac alternans would not be uniform in patients with cardiomyopathy. We further hypothesized that the spatial distribution of intracardiac alternans would influence the measurement of surface TWA. To test this hypothesis, the spatial and temporal distribution of repolarization alternans was measured along the JT interval from multiple sites in the anteroseptal right ventricular (RV) endocardium and left ventricular (LV) epicardium where wall motion abnormalities were present, indicating myocardial disease. Spectral analysis of the unipolar JT interval at each recording site was used to detect regional intracardiac alternans, which was then correlated with body surface TWA.

Abbreviations and Acronyms

CL = cycle length
ECG = electrocardiogram
EF = ejection fraction
H = high voltage (intracardiac recording of beat-to-beat fluctuations)
L = low voltage (intracardiac recording of beat-to-beat fluctuations)
LV = left ventricle/ventricular
RV = right ventricle/ventricular
TWA = T-wave alternans

Methods

Study patients. Consecutive patients with cardiomyopathy, defined as an LV ejection fraction (EF) ≤40%, and wall motion abnormalities in the anterior wall, septum, or apex were included in the study. Left ventricular function was assessed by gated blood pool nuclear imaging (multiple gate acquisition scan [MUGA]) within 6 months of enrollment. Patients were excluded if there was a history of myocardial infarction or unstable angina in the past 3 months, decompensated congestive heart failure, uncontrolled hypertension, sustained ventricular arrhythmias, or amiodarone therapy within 3 months. All patients underwent clinical electrophysiology testing for evaluation of syncope or risk stratification for prophylactic defibrillator implantation. The study was approved by the Research Ethics Board of University Health Network and Mount Sinai Hospital, and all patients gave written, informed consent.

Intracardiac recording and pacing protocol. The clinical electrophysiology study was performed in the postabsorptive state, and beta-blockers and antiarrhythmic drugs were held for 5 half lives. The research protocol commenced 30 min after the clinical electrophysiology study. Ten unipolar recordings from the RV endocardium were obtained with a 10-pole catheter (Livewire, St. Jude Medical Diagnostic Division Inc., Minnetonka, Minnesota) placed along the anteroseptal RV endocardium. Sixteen unipolar recordings from the LV epicardium were obtained from a 16-pole catheter (Pathfinder, Cardima, Freemont, California) advanced down the great cardiac vein onto the anteroseptal LV epicardium as previously described by our group (16). Both catheters have electrode pairs with 2-mm interelectrode spacing, and adjacent electrode pairs are separated by a distance of 5 mm for the Livewire and 6 mm for the Pathfinder.

Constant right atrial pacing was performed with a quadripolar catheter (Biosense Webster, Diamond Bar, California) at cycle lengths (CL) of 800, 600, and 500 ms for 2 to 4 min at each CL. During atrial pacing, simultaneous surface 12-lead electrocardiograms (ECGs) and intracardiac unipolar electrograms were recorded at a sampling rate of 1,000 Hz on a Prucka workstation (GE Medical Systems, Milwaukee, Wisconsin). The unipolar electrograms were recorded with a bandpass filter of 0.05 to 500 Hz, and Wilson central terminal provided a reference.

Repolarization alternans. Intracardiac repolarization alternans and body surface TWA were measured from unipolar electrograms and surface ECGs, respectively, with custom interactive software written in Matlab (MathWorks, Inc., Natick, Massachusetts). The last available sequence of 64 contiguous beats without ectopics, fusion beats, or loss of capture was selected for analysis of both intracardiac and body surface alternans. After QRS complex detection, baseline wander was removed by subtracting an interpolated cubic spline. The QRS complex alignment was refined by maximizing the dot product to an averaged QRS complex template (17). A 2-dimensional matrix was constructed with 64 rows corresponding to the 64 beats and n columns, where n represented the number of time points in the JT interval. Fast Fourier Transform was applied to unwindowed voltage series column-wise to generate power spectra for each time point, which were then summed to generate an aggregate power spectrum. The spectral magnitude at a frequency of 0.5 cycles/beat represents the alternans magnitude ($P_{0.5}$). The noise band was defined as the 10 preceding spectral points (0.33 to 0.48 cycles/beat) (17). The mean amplitude in this interval was the mean noise (μ_{noise}) and the SD of noise was σ_{noise}. The magnitude of alternans was measured by V_{alt} and k value (18):

$$V_{alt} = \sqrt{\{(P_{0.5} - \mu_{noise})/\text{JT duration}\}}$$

$$k = (P_{0.5} - \mu_{noise})/\sigma_{noise}$$

The presence of significant alternans at each intracardiac recording site was determined on the basis of a k value ≥3, indicating an alternans magnitude exceeding the mean noise level by more than 3 SDs (6,19). The V_{alt} was not considered in the definition of significant intracardiac alternans because there is no clinically validated threshold that

identifies a patient population at high risk of clinical events, unlike the V_{alt} (≥1.9 μV) in body surface alternans recordings (4,5). For each pacing study, intracardiac alternans was present if at least 1 intracardiac recording site had a k value ≥3. Surface TWA was present if 1 limb lead or 2 precordial leads had a k value ≥3.

Spatiotemporal distribution of intracardiac alternans. The proportion of recording sites showing alternans (k ≥3) was determined separately for the endocardium and epicardium. In addition, alternans was assessed for the apical, mid, and basal segments of the endocardium and epicardium. For this purpose, the endocardial electrodes were divided into 3 groups, namely apex (electrodes 1 to 4), mid-segment (electrodes 5 to 7), and base (electrodes 8 to 10). Similarly, epicardial electrodes 1 to 6, 7 to 11, and 12 to 16 were designated apex, mid-segment, and base, respectively. For each intracardiac recording site, temporal distribution of alternans was assessed along the JT interval. The JT interval was divided into thirds, and the presence of alternans in the early, mid, or late JT interval was indicated by a k value ≥3.

Beat-to-beat intracardiac alternans. For each intracardiac recording site, the beat-to-beat fluctuations in voltage were determined at the same time point in the JT interval that manifested the largest k value. All beats during pacing were analyzed, including the 64 beats used for spectral analysis. Alternans was defined as a pattern of alternating high (H) to low (L) voltages in at least 8 consecutive beats. A change in alternans pattern from HL to LH in the same recording electrode indicated change in alternans phase (2). The presence of alternans with an HL pattern in 1 recording electrode and an LH pattern simultaneously in another recording electrode from the same site (endocardium or epicardium) indicated discordant alternans (20).

Statistical analysis. Continuous variables are presented as mean ± SEM. Repolarization alternans was expressed as both a continuous variable (V_{alt}) and dichotomous categorical variable ("present" if k ≥ 3 vs. "absent" if k < 3). The Friedman test was used to compare V_{alt} at multiple pacing rates within the same group. Categorical variables were compared between groups with the chi square test with the Yate's correction for continuity. The Cochran Q test was used to compare repeated measures of categorical variables within the same group. A 2-tailed p value ≤0.05 was considered statistically significant. Statistical analysis was performed with Analyse-it (Analyse-it software, Leeds, United Kingdom).

Results

Study population. The study population included 14 patients (age 59 ± 4 years, 11 men) with cardiomyopathy

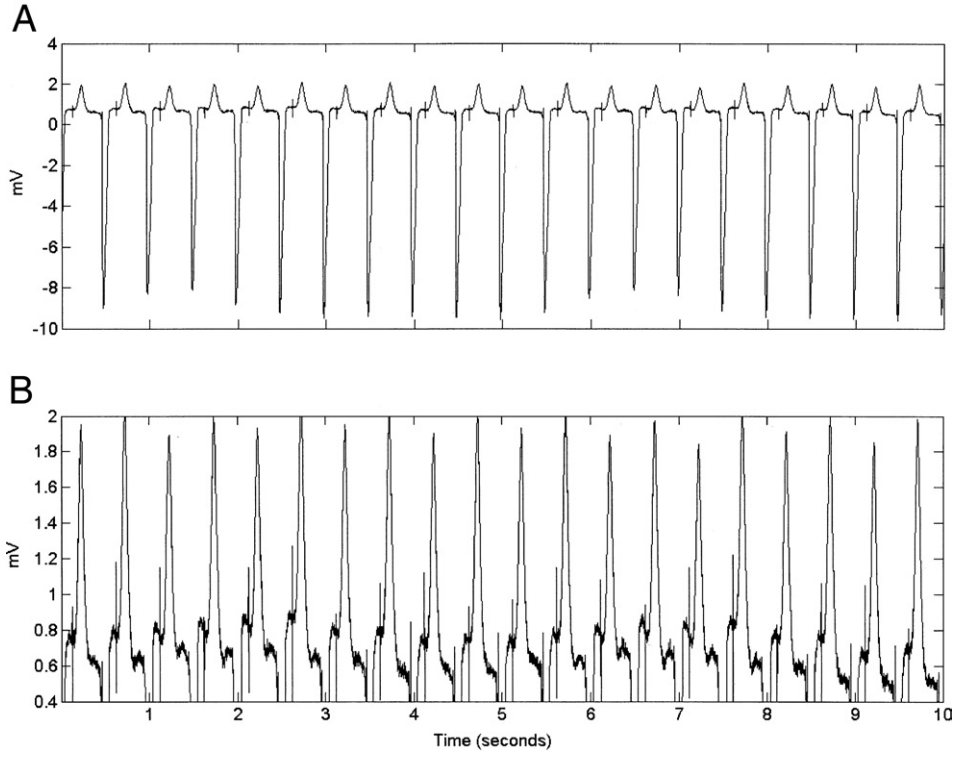

Figure 1 Intracardiac Alternans

(A) Consecutive unipolar ventricular electrograms recorded from electrode 5 (mid-segment) of the right ventricular endocardium in 1 patient during atrial pacing at cycle length 500 ms. **(B)** Magnification of the JT interval shown in **panel A** illustrates the beat-to-beat alternation of voltage.

(LVEF 29 ± 2%, RVEF 46 ± 2%). The etiology of cardiomyopathy was ischemic in 9 patients and non-ischemic in the remaining 5. No patient had a history of ventricular arrhythmias. All patients were receiving beta-blocker therapy before enrollment, and beta-blockers were held for 5 half lives before the procedure in all cases. Endocardial and epicardial recordings were available at CL 800 ms (n = 8), 600 ms (n = 13), and 500 ms (n = 13). In 6 patients, recordings at 800 ms could not be performed, owing to a higher intrinsic sinus rate. Two other patients had frequent ventricular ectopy at pacing CL 600 and 500 ms, respectively, precluding alternans analysis.

Heart rate and intracardiac alternans. Figure 1 illustrates alternans in the unipolar JT interval recorded from RV endocardial electrode 7 (mid segment) of 1 patient. Intracardiac alternans ($k \geq 3$) in at least 1 recording electrode was present in 25% of patients at CL 800 ms, and the prevalence increased to 38% at CL 600 ms and 69% at CL 500 ms ($p = 0.25$). The proportion of all recording electrodes with alternans ($k \geq 3$) was 1% at CL 800 ms, which increased to 5% at CL 600 ms and 19% at CL 500 ms ($p < 0.0001$). Among recording electrodes with alternans ($k \geq 3$), the magnitude of alternans, defined by mean V_{alt}, also increased significantly with decrease in pacing CL and measured 75 ± 7 μV at 500 ms (Table 1).

Spatial distribution of intracardiac alternans. Spatiotemporal heterogeneity of intracardiac alternans was assessed at CL 600 and 500 ms and not at CL 800 ms where only 1% of recording sites manifested alternans. The spatial distribution of alternans was not uniform. The presence of alternans varied widely from endocardium to epicardium and from apex to base in any given patient. In no patient was alternans measurable in all intracardiac recording sites. At CL 500 ms, only 19% of recording sites showed alternans. Many of the recording sites with alternans were adjacent to sites without alternans. These differences were not attributable to differing noise between recording sites, which remained uniform. The mean coefficient of variation in noise across the 10 endocardial electrodes and 16 epicardial electrodes was 22% and 24%, respectively. Figure 2 illustrates the heterogeneous apicobasal distribution of alternans in the endocardium and epicardium in 2 patients at CL 500 ms.

Table 1 Intracardiac Repolarization Alternans Prevalence and Magnitude During Atrial Pacing

	Atrial Pacing Cycle Length			
	800 ms (n = 8)	600 ms (n = 13)	500 ms (n = 13)	p Value
Pacing studies with alternans* (%)	25	38	69	0.25
Recording sites with alternans† (%)	1	5	19	<0.0001
Mean V_{alt}‡ (μV)	18 ± 3	21 ± 2	75 ± 7	<0.0001

*Proportion of pacing studies with $k \geq 3$ in any intracardiac recording electrodes; †proportion of intracardiac recording electrodes with $k \geq 3$; ‡measured from intracardiac recording electrodes with $k \geq 3$.

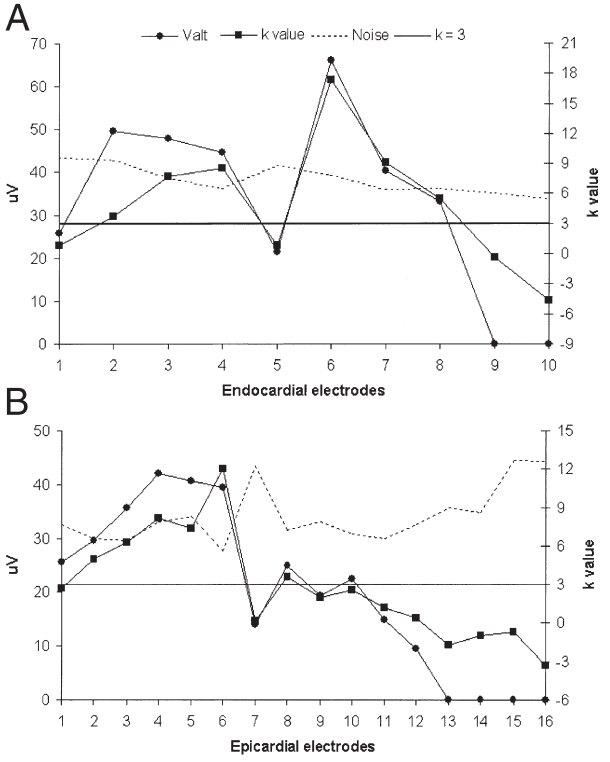

Figure 2 Spatial Heterogeneity of Alternans

Endocardial and epicardial repolarization alternans recorded from 2 patients during atrial pacing at cycle length 500 ms. The magnitude of alternans, defined by V_{alt} and k values, varies between recording electrodes, whereas the noise level remains similar. The **horizontal line** corresponds to $k = 3$, which is the threshold for the detection of significant alternans. **(A)** In the right ventricular endocardium, alternans is present at electrodes 2, 3, 4, 7, and 8. The remaining endocardial electrodes do not manifest alternans and lie adjacent to electrodes with alternans in some cases. **(B)** In the left ventricular epicardium, alternans is present at electrodes 2, 3, 4, 5, 6, and 8. In the remaining epicardial electrodes, no alternans is detected and some of these electrodes are juxtaposed next to alternating sites.

Alternans was more prevalent in the recording sites along the epicardium than endocardium at CL 600 ms (8.1% vs. 0.8%, $p = 0.008$), but no significant difference was present at CL 500 ms (21% vs. 17%, $p = 0.45$). Although spatial heterogeneity along the apex, mid-segment, and base was present in each patient with alternans, there was no consistent pattern to the spatial distribution of alternans among all patients. Thus, the proportion of recording sites with alternans in the apex, mid-segment, and base were similar for the endocardium (15% vs. 23% vs. 13%, $p = 0.45$) and epicardium (24% vs. 16% vs. 16%, $p = 0.18$) at CL 500 ms. Apicobasal differences at CL 600 ms were not determined, owing to the limited number of recording sites with alternans in each segment.

Temporal distribution of intracardiac alternans. Alternans was not uniformly distributed along the JT interval in

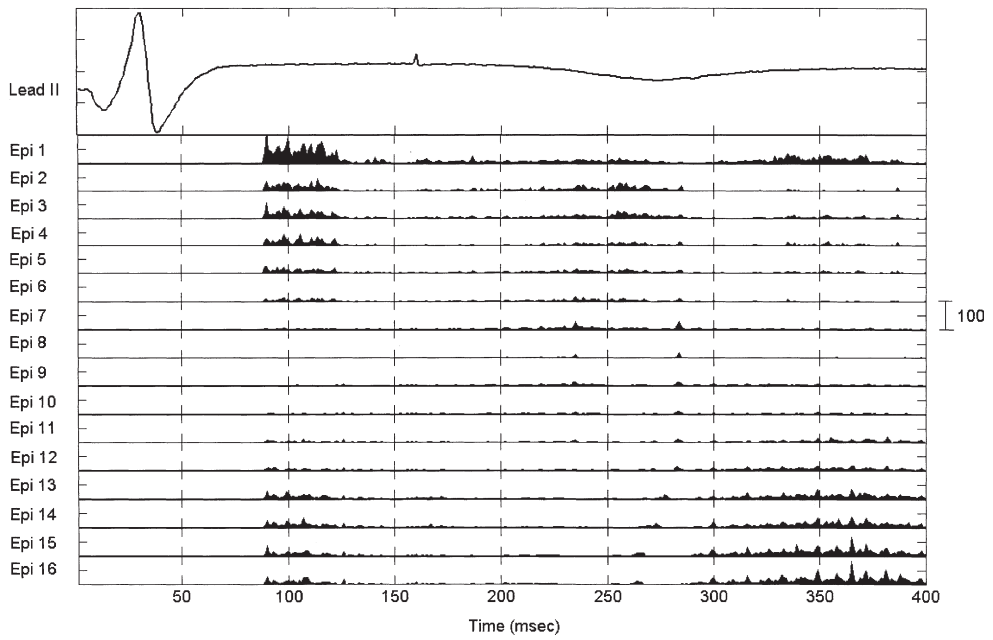

Figure 3 **Temporal Heterogeneity of Alternans**

Epicardial repolarization alternans recorded from 1 patient during atrial pacing at cycle length 600 ms. A surface QRS complex and JT segment from lead II is shown at the **top**. The k value is plotted as a function of the JT interval for all 16 epicardial electrodes (Epi) along the anteroseptal ventricle.

any particular recording site, implying temporal heterogeneity within the repolarization phase. Moreover, temporal distribution of alternans differed across the apicobasal epicardium and endocardium for each patient. Figure 3 illustrates temporal heterogeneity in the magnitude of alternans at CL 500 ms. In this patient, alternans is pronounced in the early JT interval of the apical epicardium as well as the late JT interval of the basal segments. Among all patients, the differences in temporal distribution of alternans between recording electrodes resulted in apicobasal spatial heterogeneity that was not apparent when the entire JT interval was analyzed. When alternans was computed separately for each third of the JT segment at CL 500 ms, apical alternans distributed predominantly in the early and mid JT segments rather than the late JT segment. As a consequence, the proportion of recording sites with late JT alternans was significantly smaller at the apex when compared with the basal or mid segments (Fig. 4).

Alternans phase reversal and discordance. Alternans phase reversal was recorded in 5 pacing studies. In each case, a spontaneous premature beat induced phase reversal. The phase reversal resulted in concordant alternans in 4 studies such that all recording electrodes with alternans had the same alternans phase. In one study, phase reversal resulted in discordant alternans, as illustrated in Figure 5. In this study, phase reversal was localized to epicardial electrodes 2 to 5, but not epicardial electrode 1, thereby producing discordant alternans between these 2 recording sites.

Discordant alternans was observed in an additional 4 studies after a spontaneous premature beat (n = 2) or shortly after the onset of pacing at CL 500 ms (n = 2) (Table 2). Discordance in all 5 pacing studies was limited to the epicardium, and in 4 studies, the discordance was observed between the apex and base. Figure 6 shows discordant alternans involving the epicardial apex and base that began shortly after pacing. The mid segment in this patient does not alternate and represents a node.

Relationship of surface alternans to intracardiac alternans. Alternans was present on the body surface in 5 pacing studies at CL 500 ms (n = 4) and CL 600 ms (n = 1). The mean surface V_{alt} in these studies was 14 ± 8 μV. Body surface TWA was always associated with intracardiac alternans in at least 1 of the recording electrodes. However, intracardiac alternans was sometimes present without measurable surface TWA. To determine the relationship between surface TWA and intracardiac alternans, 2 groups were compared. Group 1 comprised the 5 (15%) pacing studies with both intracardiac alternans and surface TWA. Group 2 consisted of 11 (32%) pacing studies with intracardiac alternans but no surface TWA. The proportion of intracardiac recording sites with alternans was significantly greater in Group 1 (38 ± 15%) compared with Group 2 (17 ± 5%, $p < 0.005$). When a cutoff of 18% was used, which represented the proportion of intracardiac recording sites with alternans, the sensitivity in identifying pacing studies with surface alternans was 80% and the specificity was 73%.

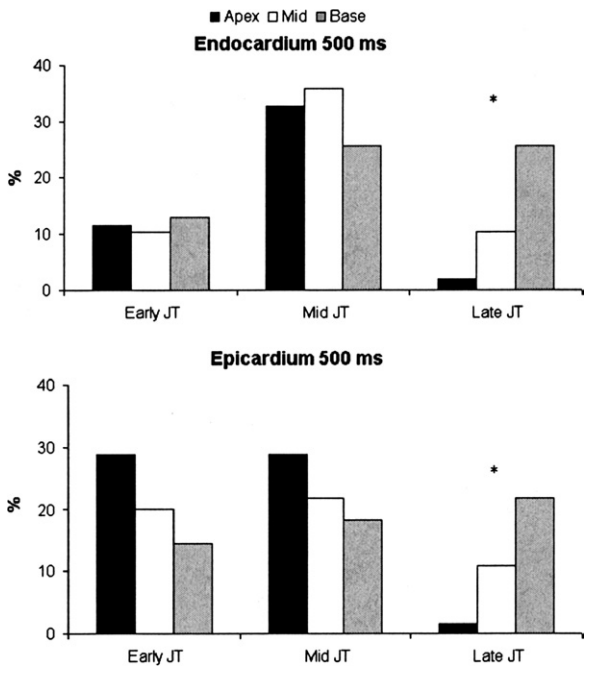

Figure 4 **Apicobasal Alternans**

Apicobasal differences in endocardial and epicardial repolarization alternans during atrial pacing at cycle length 500 ms. The proportion of recording sites with alternans is compared between apical, mid, and basal segments. Alternans is measured separately for each third of the JT interval denoted as early JT, mid JT, and late JT. *$p < 0.05$ (apex vs. mid vs. base).

Discussion

The major finding of this study is that the spatial and temporal distribution of repolarization alternans is not uniform along the endocardium and epicardium of patients with cardiomyopathy. In addition, phase reversal and discordant alternans are present in these patients. A larger spatial distribution of intracardiac alternans is associated with measurable body surface TWA. This is the first study, to our knowledge, in which repolarization alternans has been simultaneously measured from multiple intracardiac locations and the body surface in humans. The unipolar recordings of the JT interval permitted evaluation of regional alternans, which has been used previously in animal models of ischemia (9).

Alternans magnitude and spatiotemporal heterogeneity. The magnitude of intracardiac alternans was rate-dependent, and the proportion of pacing studies with significant alternans increased at higher pacing rates. Rate dependence has also been demonstrated with body surface TWA recordings (1). The magnitude of intracardiac alternans was up to 10-fold higher than that recorded on the body surface. When the endocardium and epicardium were compared, a greater number of epicardial sites manifested alternans at CL 600 ms, but no significant differences were seen at CL 500 ms. This suggests that the heart rate threshold for development of alternans is lower in the epicardium. The mechanism for this observation is speculative, but greater epicardial alternans might be due to more extensive epicardial disease, particularly in our patients with ischemic cardiomyopathy who had predominantly LV dysfunction and preserved RV function. Abnormal intracellular calcium cycling has been implicated in the pathogenesis of alternans (8,21), and impaired cardiomyocyte calcium homeostasis has been demonstrated in heart failure (13). Thus, diseased myocytes in the LV epicardium might demonstrate alternans at lower heart rates than their healthier counterparts in the RV.

Temporal heterogeneity of alternans was present along the JT interval. Although the majority of patients had alternans clustered in the middle third of the JT interval, several recording sites in the same patient manifested alternans in both the early and late portion of the JT interval. Early JT alternans was not due to late depolarization alternans, because it extended 100 ms beyond the end of the QRS complex. This multimodal distribution of intracardiac alternans has also been observed by Christini et al. (6) with a single RV endocardial recording site. In our study, the temporal distribution of alternans along the JT interval also varied between recording electrodes, which has

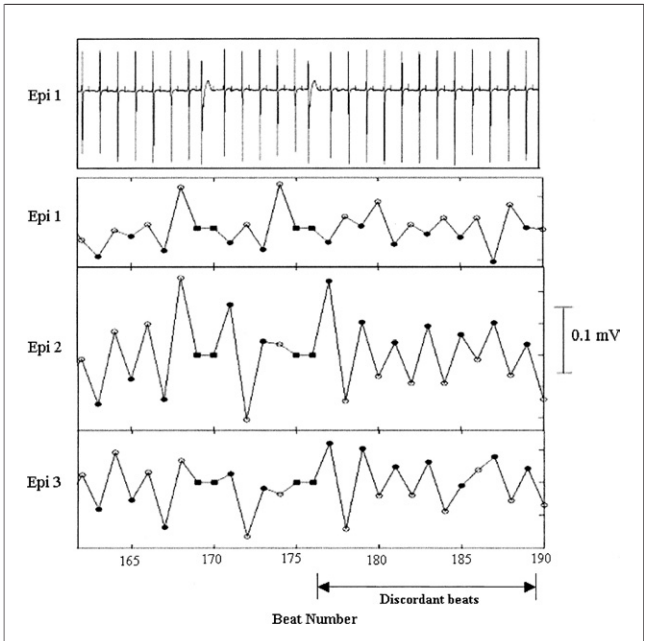

Figure 5 **Discordance With Ectopics**

Discordant alternans initiated by ectopic beats in 1 patient. The **top tracing** shows unipolar ventricular electrograms from epicardial electrode (Epi) 1 during atrial pacing at cycle length 600 ms. Note the 2 spontaneous ectopic beats. The **bottom 3 tracings** show the corresponding beat-to-beat voltages (at identical time points in the JT interval) for epicardial electrodes 1 to 3. The odd and even beats are indicated by **open circles** and **filled circles**, respectively. The ectopic beat and the preceding beat are replaced with an average of the other beats and are indicated by a **filled square**. After the second ectopic beat **(square)**, discordant alternans develops between electrode 1 and electrodes 2 to 3.

Table 2 Episodes of Discordant Intracardiac Alternans

Patient	Pacing CL (ms)	Initiation of Discordance	Discordant Recording Sites*		Duration of Discordance (beats)
			Site 1	Site 2	
1	500	Onset of pacing	Epi 1–4	Epi 12–16	240
2	500	Ventricular ectopic	Epi 1–9	Epi 13–16	40
3	500	Ventricular ectopic	Epi 1–2	Epi 5–16	50
4	600	Ventricular ectopic	Epi 1	Epi 2–5	13
5	500	Onset of pacing	Epi 1–4	Epi 11–16	24

*Low voltage to high voltage (LH) alternans at recording site 1 versus high voltage to low voltage (HL) alternans at recording site 2.
CL = cycle length; Epi = epicardial electrode.

not been previously reported. Apical alternans was distributed in the early and mid JT segment rather than the late JT segment, resulting in significantly less apical alternans in the late JT segment. The basis for this observation is unclear. Nearing et al. (15) found alternans restricted to the first half of the T wave in an animal model of ischemia. It is thus possible that the earlier distribution of alternans in the apical segments could be due to subclinical ischemia in this region during rapid pacing.

Alternans phase reversal and discordance. Spatiotemporal patterns of alternans are dynamic, as evidenced by phase reversal after ectopic beats in our study. Phase reversal in all myocardial segments with alternans resulted in concordant alternans, whereas incomplete phase reversal caused discor-

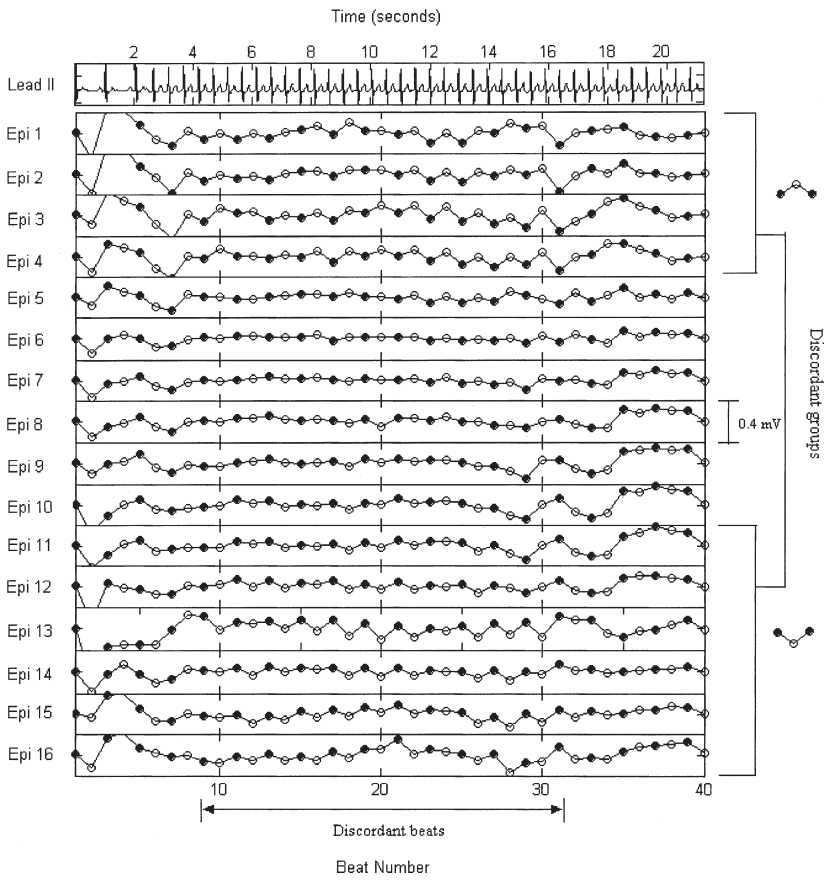

Figure 6 Discordance With Heart Rate Acceleration

Discordant alternans initiated by heart rate acceleration in 1 patient. The **top tracing** shows surface electrocardiogram lead II at the commencement of atrial pacing at cycle length 500 ms. The **bottom tracings** show the beat-to-beat voltages (at identical time points in the JT interval) for epicardial electrodes (Epi) 1 to 16. This sequence begins with the last 2 sinus beats before pacing begins. The even and odd beats are indicated by an **open circle** and a **filled circle**, respectively. Discordant alternans between the apical (Epi 1 to 4) and basal electrodes (Epi 11 to 16) begins at the 10th beat and lasts for 24 beats. The intervening electrodes in the mid segment represent a node without alternans.

dant alternans. All episodes of discordant alternans were initiated either by an ectopic beat or rapid pacing. These observations have been predicted in theoretical models of discordant alternans (22). In our patients, the apex and base were the most common sites of discordance separated by a node. Pastore et al. (10) also observed discordant alternans between the apex and base along with an intervening node in the guinea pig heart with optical mapping. The mechanism for discordance in the human heart is unclear, but spatial heterogeneity of intracellular calcium cycling (8) or restitution kinetics (12) have been implicated in theoretical models and animal experiments. In the absence of tissue heterogeneity, discordance can also arise from the interaction between conduction velocity restitution and action potential duration restitution (22). In these studies, ectopic beats or rapid pacing can initiate discordant alternans and the resulting steep repolarization gradients often trigger ventricular fibrillation (10).

Implications for arrhythmogenesis. Although arrhythmogenic repolarization gradients can arise from discordant alternans, these gradients might also develop in the face of spatiotemporal alternans heterogeneity. In our study, several patients demonstrated localized regions of alternans that were adjacent to nonalternating segments. This finding corresponds with the experimental findings that alternans is often circumscribed. Pruvot et al. (8) found regional differences in the onset of alternans in the guinea pig heart that corresponded to regional differences in calcium handling. Sutton et al. (23) also described alternans as a localized phenomenon on the epicardial surface of the human heart during intraoperative mapping. As a consequence, large voltage gradients might develop between alternating and nonalternating segments, potentially creating functional conduction block that presages re-entry.

Intracardiac and surface alternans. Intracardiac alternans will project onto the body surface. Clinical studies comparing surface and intracardiac alternans have used only a single RV endocardial site, and no consistent relationship has been observed (6,7). With multisite intracardiac recordings in our study, we found that intracardiac alternans was always present in studies with surface TWA. The presence of surface TWA was related to the number of alternating intracardiac recording sites. If 18% or more of intracardiac recording sites manifested alternans, surface TWA was detectable with high sensitivity and specificity.

Clinical implications. Although the magnitude of intracardiac alternans is greater than surface TWA, a single recording site might have limited sensitivity in detecting alternans in the presence of spatial heterogeneity. Thus, the detection of intracardiac alternans with an implantable cardioverter defibrillator lead in the RV (24) might underestimate alternans at remote sites.

Surface TWA has been shown to be an important risk stratifier in patients with cardiomyopathy, but the positive predictive value is poor (4). The assessment of spatiotemporal alternans heterogeneity, including the detection of discordance, from intracardiac recordings might improve the prognostic utility of alternans in these patients, which merits further investigation.

Study limitations. Measurement of intracardiac alternans was limited to the anteroseptal RV and LV, and other regions were not simultaneously sampled owing to the technical constraints of using more than 2 transvenous recording catheters. Second, the pacing CLs in the study differed from CL 550 ms used to assess surface TWA. The CL 500 ms increased the proportion of recording sites with alternans when compared with CL 550 ms, thereby permitting assessment of spatiotemporal alternans heterogeneity while still being tolerable for the patients with ventricular dysfunction. Third, the correlation of intracardiac alternans with clinical events was not studied and will require a larger sample size and long-term follow-up.

Conclusions. Spatial differences in the magnitude, temporal distribution, and phase of alternans exist in patients with cardiomyopathy. Greater spatial distribution of intracardiac alternans is associated with measurable body surface TWA. Spatiotemporal alternans heterogeneity might create large repolarization gradients in cardiomyopathy patients, thereby providing the arrhythmogenic substrate for re-entrant ventricular arrhythmias.

Acknowledgments

The authors thank the nursing staff of the Clinical Cardiovascular Research Laboratory of Mount Sinai Hospital for their help in the completion of these studies.

Reprint requests and correspondence: Dr. Vijay S. Chauhan, PMCC 3-503, Toronto General Hospital, 150 Gerrard Street West, Toronto, Ontario, M5G 2C4 Canada. E-mail: vijay.chauhan@uhn.on.ca.

REFERENCES

1. Kaufman ES, Mackall JA, Julka B, Drabek C, Rosenbaum DS. Influence of heart rate and sympathetic stimulation on arrhythmogenic T wave alternans. Am J Physiol Heart Circ Physiol 2000; 279:H1248–55.
2. Narayan SM, Lindsay BD, Smith JM. Demonstration of the proarrhythmic preconditioning of single premature extrastimuli by use of the magnitude, phase, and distribution of repolarization alternans. Circulation 1999;100:1887–93.
3. Narayan SM, Smith JM. Differing rate dependence and temporal distribution of repolarization alternans in patients with and without ventricular tachycardia. J Cardiovasc Electrophysiol 1999;10:61–71.
4. Bloomfield DM, Steinman RC, Namerow PB, et al. Microvolt T-wave alternans distinguishes between patients likely and patients not likely to benefit from implanted cardiac defibrillator therapy: a solution to the multicenter automatic defibrillator implantation trial (MADIT) II conundrum. Circulation 2004;110:1885–9.
5. Bloomfield DM, Bigger T, Steinman RC, et al. Microvolt T-wave alternans and the risk of death or sustained ventricular arrhythmias in patients with left ventricular dysfunction. J Am Coll Cardiol 2006;47: 456–63.
6. Christini DJ, Stein KM, Hao SC, et al. Endocardial detection of repolarization alternans. IEEE Trans Biomed Eng 2003;50:855–62.
7. Paz O, Zhou X, Gerez T, et al. T wave alternans detected from implantable cardioverter defibrillator electrograms (abstr). Heart Rhythm 2005;2:S31–2.

8. Pruvot EJ, Katra RP, Rosenbaum DS, Laurita KR. Role of calcium cycling versus restitution in the mechanism of repolarization alternans. Circ Res 2004;94:1083–90.
9. Carson DL, Cardinal R, Savard P, Vermeulen M. Characterisation of unipolar waveform alternation in acutely ischaemic porcine myocardium. Cardiovasc Res 1986;20:521–7.
10. Pastore JM, Girouard SD, Laurita KR, Akar FG, Rosenbaum DS. Mechanism linking T-wave alternans to the genesis of cardiac fibrillation. Circulation 1999;99:1385–94.
11. Qian YW, Clusin WT, Lin SF, Han J, Sung RJ. Spatial heterogeneity of calcium transient alternans during the early phase of myocardial ischemia in the blood-perfused rabbit heart. Circulation 2001;104:2082–7.
12. Chinushi M, Kozhevnikov D, Caref EB, Restivo M, El-Sherif N. Mechanism of discordant T wave alternans in the in vivo heart. J Cardiovasc Electrophysiol 2003;14:632–8.
13. Piacentino V 3rd, Weber CR, Chen X, et al. Cellular basis of abnormal calcium transients of failing human ventricular myocytes. Circ Res 2003;92:651–8.
14. Nash MP, Bradley CP, Sutton PM, et al. Whole heart APD restitution properties in cardiac patients: a combined clinical and modelling study. Exp Physiol 2006;91:339–54.
15. Nearing BD, Huang AH, Verrier RL. Dynamic tracking of cardiac vulnerability by complex demodulation of the T wave. Science 1991; 252:437–40.
16. Chauhan VS, Downar E, Nanthakumar K, et al. Increased ventricular repolarization heterogeneity in patients with ventricular arrhythmia vulnerability and cardiomyopathy: a human in vivo study. Am J Physiol Heart Circ Physiol 2006;290:H79–86.
17. Narayan SM, Smith JM. Spectral analysis of periodic fluctuations in electrocardiographic repolarization. IEEE Trans Biomed Eng 1999; 46:203–12.
18. Rosenbaum DS, Jackson LE, Smith JM, Garan H, Ruskin JN, Cohen RJ. Electrical alternans and vulnerability to ventricular arrhythmias. N Engl J Med 1994;330:235–41.
19. Smith JM, Clancy EA, Valeri CR, Ruskin JN, Cohen RJ. Electrical alternans and cardiac electrical instability. Circulation 1988;77: 110–21.
20. Nearing BD, Verrier RL. Analysis of complex T-wave oscillations for prediction of ventricular fibrillation. J Electrocardiol 2003;36 Suppl: 199–203.
21. Walker ML, Wan X, Kirsch GE, Rosenbaum DS. Hysteresis effect implicates calcium cycling as a mechanism of repolarization alternans. Circulation 2003;108:2704–9.
22. Watanabe MA, Fenton FH, Evans SJ, Hastings HM, Karma A. Mechanisms for discordant alternans. J Cardiovasc Electrophysiol 2001;12:196–206.
23. Sutton PM, Taggart P, Lab M, Runnalls ME, O'Brien W, Treasure T. Alternans of epicardial repolarization as a localized phenomenon in man. Eur Heart J 1991;12:70–8.
24. Maybhate A, Hao SC, Iwai S, et al. Detection of repolarization alternans with an implantable cardioverter defibrillator lead in a porcine model. IEEE Trans Biomed Eng 2005;52:1188–94.